Heterogeneous Catalysis

DOI: 10.1002/ange.201106702

Design of a Highly Active Ir/Fe(OH)$_x$ Catalyst: Versatile Application of Pt-Group Metals for the Preferential Oxidation of Carbon Monoxide**

Jian Lin, Botao Qiao, Jingyue Liu, Yanqiang Huang, Aiqin Wang, Lin Li, Wansheng Zhang, Lawrence F. Allard, Xiaodong Wang, and Tao Zhang**

The proton-exchange membrane fuel cell (PEMFC) has been regarded as one of the most promising candidates for the efficient use of hydrogen energy.[1] However, small amounts of CO (0.3–1%) in the H_2 stream from reforming processes must be selectively removed because CO is highly poisonous to the Pt anode of a PEMFC.[2] The preferential oxidation of CO in a H_2-rich gas (PROX) is presently the most effective approach to address this problem.[3] Oxide-supported Au catalysts are highly active for the PROX reaction even at room temperature,[4] but the lower stability and sensitivity to CO_2 constrain their practical applications. Supported Pt catalysts, on the other hand, are less active[5] and only a few have shown reasonable activity for conversion of CO at temperatures lower than 60 °C.[6] Therefore, it is highly desirable to develop improved catalysts with better catalytic performance for the PROX reaction at lower temperatures.

Ir has a higher melting point and surface energy than other metals with 5f orbitals, such as Pt and Au, and Ir can be well-dispersed on and strongly interact with the support.[7] However, compared to Pt- and Au-based catalysts, Ir-based catalysts have limited applications in heterogeneous catalysis[7b] and are rarely investigated for the PROX reaction, most probably because of its inferior activity. Although much effort has been made to improve the activity of Ir-based catalysts and remarkable progress has been achieved,[8] their activities for the PROX reaction are still low at low temperatures. In fact, there is no report so far claiming that Ir-based catalysts can show high activity at temperatures below 80 °C; thus it remains a formidable challenge to utilize Ir-based catalysts for the PROX reaction at ambient temperatures.

One basic task of modern catalysis is to rationally design catalysts based on the fundamental understanding of their reaction mechanisms.[9] Especially, the contribution of support materials to the performance of the final catalysts should be taken into account.[10] For the PROX reaction, the strong binding of CO to Ir poisons the surface so that O_2 cannot competitively adsorb on the Ir surface and be activated at low temperatures, thereby prohibiting the conversion of CO to CO_2. Therefore, weakening the adsorption strength of CO and/or promoting the activation of O_2 at lower temperatures have become the crucial steps. Ferric oxide has proven effective for O_2 activation and has been used extensively as an additive to Pt-based catalysts.[3a,11] Recently, we have designed a bimetallic catalyst by adding FeO_x to a supported Ir catalyst, and the activity for the PROX reaction was improved.[8c,12] Further study of the catalytic reactions showed that the reaction rate of CO oxidation correlated well with the presence and amount of Fe^{2+}, suggesting that Fe^{2+} sites were indeed the active sites for O_2 activation.[13] The coordinatively unsaturated Fe center was also recently identified as the site to activate O_2, which helped the design of a highly active $FeO_x/Pt/SiO_2$ catalyst to totally convert CO at room temperature.[6d] All of these studies suggest that the presence of low-valent Fe (Fe^{2+}) played a decisive role in improving the PROX activity, thus providing a clue for obtaining a highly effective Ir-based catalyst by incorporating materials containing, or easily forming, Fe^{2+} species.

Ferric hydroxide (Fe(OH)$_x$) is a novel support material which has recently been adopted to stabilize various types of metal species for CO oxidation.[14] It possesses a large surface area and a large amount of OH^- groups; these unique properties make Fe(OH)$_x$ a good candidate for generating highly dispersed metal clusters or even single-atom catalysts.[15] Furthermore, the longer Fe–O bonds in Fe(OH)$_x$ (compared to those in Fe_2O_3) make it easier to form Fe^{2+} species during the reduction processes,[16] even around room temperatures (< 50 °C).[17] We expect that properly synthesized Ir/Fe(OH)$_x$ catalysts should be highly active for the PROX reaction. In this work, we prepared a novel Ir/Fe(OH)$_x$

[*] Dr. J. Lin,[+] Dr. B. Qiao,[+] Dr. Y. Huang, Prof. Dr. A. Wang, Dr. L. Li, Dr. W. Zhang, Prof. Dr. X. Wang, Prof. Dr. T. Zhang
State Key Laboratory of Catalysis
Dalian Institute of Chemical Physics
Chinese Academy of Sciences, Dalian 116023 (China)
E-mail: taozhang@dicp.ac.cn
xdwang@dicp.ac.cn
Homepage: http://www.taozhang.dicp.ac.cn/

Prof. Dr. J. Liu
Center for Nanoscience
Department of Physics & Astronomy
and Department of Chemistry and Biochemistry
University of Missouri-St. Louis
One University Boulevard, St. Louis, MO 63121 (USA)

Dr. L. F. Allard
Materials Science and Technology Division
Oak Ridge National Laboratory, Oak Ridge, TN 37831 (USA)

[+] These authors contributed equally to this work.

[**] Financial supports for this research work from the NSF of China (grant numbers 20803079, 21003119, 21076211, and 21103173). The electron microscopy work was conducted at the Oak Ridge National Laboratory's High Temperature Materials Laboratory, sponsored by the U. S. Department of Energy, Office of Energy Efficiency and Renewable Energy, Vehicle Technologies Program.

Supporting information for this article is available on the WWW under http://dx.doi.org/10.1002/anie.201106702.

catalyst by a co-precipitation method and found that it indeed provided a high activity for the PROX reaction with a total conversion of CO at temperatures between 20–60 °C. The turnover frequency (TOF) of this catalyst is comparable to that of the standard gold catalyst (provided by the World Gold Council, WGC). Our approach to catalyst design can be extended to preparation of other noble-metal catalysts, for example, Pt and Rh. Thus we believe that such a design strategy is general and other $Fe(OH)_x$-supported noble-metal catalysts should provide improved activity for the PROX reaction.

An $Fe(OH)_x$-supported Ir catalyst with a 2.4 wt% of Ir loading was obtained by co-precipitation of an aqueous solution of H_2IrCl_6 and $Fe(NO_3)_3$ in an aqueous solution of NaOH, similar to the procedure for preparing the Ir–CeO_2 catalyst reported previously (see the Supporting Information for more details on the sample preparation).[18] The as-synthesized sample dried at 80 °C without calcination hereafter is denoted as Ir/Fe-UC, and those calcined at 200 °C or 400 °C are denoted as Ir/Fe-C2 or Ir/Fe-C4, respectively.

The Ir loading level in the Ir/Fe-UC catalyst, measured by inductively coupled plasma spectrometry (ICP-AES, see Table S1 in the Supporting Information), is equal to the theoretical loading, indicating that there was no Ir loss during the preparation process. The Ir loading levels in the calcined samples increase slightly with the calcination temperature because of weight loss of the $Fe(OH)_x$ support. Correspondingly, the BET surface areas of the calcined catalysts decrease with increasing calcination temperature. However, even after calcination at 400 °C, this catalyst still possesses a very large surface area (192 $m^2 g^{-1}$).

Figure 1 a illustrates the profiles of CO conversions for the PROX reaction as a function of reaction temperature. Prior to the activity test, all the catalysts except Au/Fe_2O_3-WGC were pre-reduced at 200 °C in a flow of 20 mL min^{-1} of 10% H_2 in He for 30 min. The 4.4 wt% Au/Fe_2O_3-WGC catalyst, which is well-known for its high activity for oxidation of CO,[19] was tested first to benchmark the activity measurement system. The conversions of CO on this sample reach 100% at temperatures between 20–40 °C and then decrease gradually with reaction temperature because of the competitive oxidation of H_2. For comparison, we also tested a conventional Ir/SiO_2 catalyst (3.0 wt%) prepared by an impregnation method. The CO conversion is negligible at room temperature and is only about 38% at 100 °C. On the other hand, our Ir/Fe-UC and Ir/Fe-C2 catalysts yield a total conversion of CO at ambient temperature; they are as active as the Au/Fe_2O_3-WGC catalyst and provide an activity significantly higher than that of the Ir/SiO_2 catalyst. Furthermore, the temperature ranges for achieving 100% conversion of CO (20–60 and 20–50 °C, respectively) are much wider than that of the Au/Fe_2O_3-WGC catalyst. A wider temperature range for complete CO oxidation is considered to improve the operational flexibility for practical applications. Although Ir/Fe-C4 is less active than Ir/Fe-UC and Ir/Fe-C2, it still provides a total conversion of CO at temperatures between 40–60 °C. Our Ir/Fe catalysts contain only about half the amount of noble-metal loading compared to the Au/Fe_2O_3-WGC catalyst. As far as we know, our Ir/Fe-UC catalyst is the most active and selective Ir-based catalyst reported in the literature, and is even higher than or at least comparable to the most active supported Pt catalyst reported previously (see Table S2 in the Supporting Information).

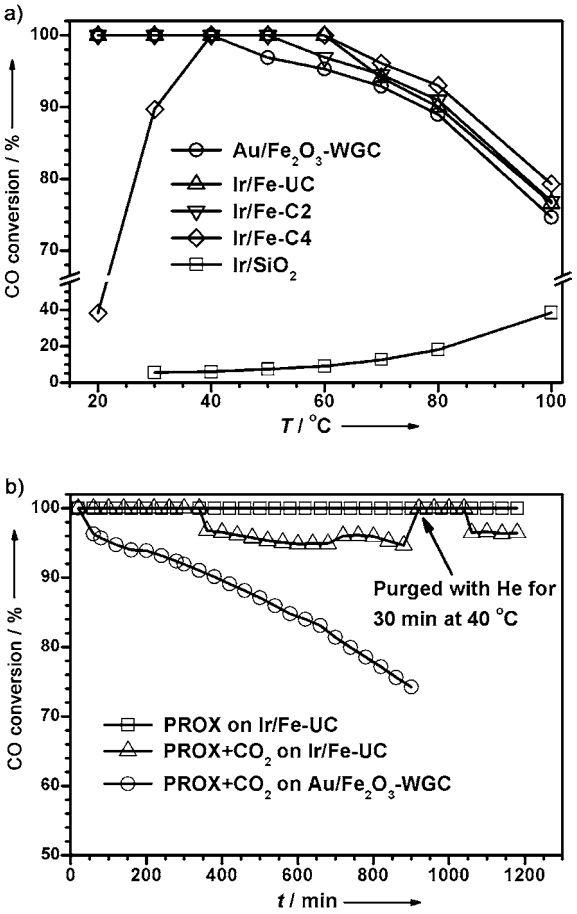

Figure 1. Conversion of CO as a function of a) the reaction temperature and b) the reaction time at 40 °C over Ir/$Fe(OH)_x$ and Au/Fe_2O_3-WGC catalysts. Reaction conditions: 1 vol% CO, 1 vol% O_2, 40 vol% H_2 (in some cases addition of 20 vol% CO_2), and balance He. Weight hourly space velocity (WHSV): 18000 mL h^{-1} g_{cat}^{-1}.

The activity decreases with the Ir loading (see Figure S1 in the Supporting Information): when the Ir loading decreases to 1.2 wt%, the temperature range for complete oxidation of CO shifts to 40–70 °C and with a 0.7 wt% Ir loading the conversion rate for CO does not reach 100% even at 100 °C. This result indicates that the temperature ranges for the total conversion of CO could be adjusted, to a certain extent, by varying the Ir loading. It also suggests that Ir clusters or nanoparticles affect the behaviour and performance of the catalysts.

To further show the surprisingly high activity of these Ir/Fe catalysts, we measured the specific rate and turnover frequency (TOF) at 27 °C and 80 °C (the typical working temperature of PEMFC) under differential conditions (the conversions of CO were maintained below 20%). As shown in Table 1, either the specific rate for the oxidation of CO over Ir/Fe-UC (0.15 mol_{co} h^{-1} g_{Ir}^{-1}) or the TOF (calculated with the dispersion of Ir; 3.03×10^{-2} s^{-1}), is only slightly lower than that of Au/Fe_2O_3-WGC (0.22 mol_{co} h^{-1} g_{Au}^{-1} or 4.75×10^{-2} s^{-1}),

Table 1: Specific rate and turnover frequency (TOF) of Ir/Fe catalysts compared with Au- and Pt-based catalysts.

	Metal loading [wt%]	Reaction type	T [°C]	Specific rate [$mol_{co}\,h^{-1}\,g_{Ir}^{-1}$]	TOF [$10^2\ s^{-1}$][b]	Note
Au/Fe_2O_3-WGC[a]	4.4	CO oxidation	27	0.22	4.75	this work
Ir/Fe-UC	2.4	CO oxidation	27	0.15	3.03	this work
Au/Fe_2O_3-WGC[a]	4.4	PROX	27	0.39	8.60	this work
Ir/Fe-UC	2.4	PROX	27	0.48	10.00	this work
Au/Fe_2O_3-WGC[a]	4.4	PROX	80	0.80	17.60	this work
Ir/Fe-UC	2.4	PROX	80	0.66	13.80	this work
$Ir/Ce_{0.63}Zr_{0.37}O_2$	2.0	PROX	80	0.07	1.30	Ref. [8a]
Ir-in-CeO_2	5.0	PROX	100	–	4.30	Ref. [18]
Ir/SiO_2	3.0	PROX	100	0.12	0.64	Ref. [21]
Pt/Al_2O_3	0.5	PROX	80	–	0.20	Ref. [4a]
K-Pt/Al_2O_3	2.0	PROX	80	0.24	3.30	Ref. [6e]
Pt/Fe-UC	2.0	PROX	27	0.19	14.00	this work
Rh/Fe-UC	2.0	PROX	27	0.14	3.04	this work

[a] Provided by the World Gold Council. [b] The gold dispersion was calculated according to the relationship between dispersion and particle size, that is, $D=1/d_{Au}$. Ir, Pt, and Rh dispersions were measured by CO chemisorption on Auto Chem II 2920 by assuming CO/Ir, Pt, Rh = 1/1.

indicating that they possess comparable activities. For the Ir/Fe-UC catalyst, the activity for the PROX reaction is increased by two and three times compared to that for the oxidation of CO, which may be due to the promotion of the existence of H_2 or the formation of H_2O.[20] This significant enhancement indicates that Ir/Fe-UC is more suitable for the PROX than for the oxidation of CO. On the other hand, although the calcination treatment results in a decrease of the activity, Ir/Fe-C2 and Ir/Fe-C4 still give high TOF and specific rate for the PROX reaction (see Table S3 in the Supporting Information). In fact, compared with the reported Ir- and Pt-based catalysts (Table 1), our Ir/Fe-UC catalyst is at least one order of magnitude more active, unambiguously showing an extremely high activity for the PROX reaction. We have also calculated the apparent activation energies (E_a) of Ir/Fe-UC for the oxidation of CO and the PROX reaction based on the TOF values measured at different temperatures (see Figure S2 and Table S4 in the Supporting Information). It shows a low E_a of 15.4 kJ mol^{-1} for the oxidation of CO and an even lower value of 5.2 kJ mol^{-1} for the PROX reaction. The outstanding performance of our Ir/Fe-UC catalyst correlates well with the lower activation barriers for the oxidation of CO.

The presence of CO_2 in H_2 from reforming gases usually exerts a negative effect by its adsorption as carbonates during the reaction, thereby constraining the practical application of supported metal catalysts.[4b,8b,21] We tested the influence of CO_2 on this new Ir/Fe-UC catalyst through a conversion versus time mode at 40 °C and compared the result with that obtained on the Au/Fe_2O_3-WGC catalyst. As shown in Figure 1b, the conversion of CO over Ir/Fe-UC remains 100% for 1200 min at 40 °C without any decay. When 20 vol% CO_2 was added, the total conversion of CO only maintains for about 360 min, and then decreases gradually. Even so, the 95% CO conversion could further maintain for another 540 min and the complete CO conversion is recovered by purging the catalyst with He at 40 °C for 30 min. For comparison, the CO conversion on Au/Fe_2O_3-WGC catalyst begins to decay after only 30 min of contact with the reactants and with a faster decreasing rate to 75% for the conversion of CO after 900 min. Figure 1b clearly shows that our Ir/Fe-UC catalyst has a better tolerance to the poisoning by CO_2. We have also investigated the stability of our catalyst at the working temperature of PEMFC (80 °C) by greatly increasing the space velocity to avoid a conversion of 100% of CO. As shown in Figure S3 in the Supporting Information, the catalyst shows a good stability for a run of 1000 min. Moreover, with the addition of 5 vol% water vapor, both the conversion of CO and the stability are significantly promoted, indicating that the Ir/Fe-UC catalyst is also water resistant. These results show that our Ir/Fe-UC catalyst is a promising catalyst for the PROX reaction.

High-resolution transmission electron microscopy (HRTEM) and high-angle annular dark-field scanning transmission electron microscopy (HAADF-STEM) techniques were used to examine the distribution of the Ir species on Ir/Fe-UC (after reduction with 10% H_2 in He at 200 °C for 30 min) and representative images were shown in Figure 2 and Figure S4 in the Supporting Information. As expected, the Ir species are highly dispersed and too small to be detected by the HRTEM technique (Figure 2a). Lattice

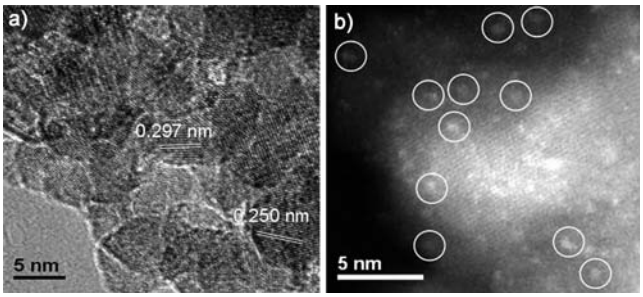

Figure 2. HRTEM and HAADF-STEM images of Ir/Fe-UC (prereduced at 200 °C for 30 min with 10% H_2 in He).

fringes with spacings of 0.297 and 0.251 nm corresponding to the (220) and (311) planes of Fe_3O_4, respectively, are clearly shown, indicating that the support changed to Fe_3O_4. This conclusion is corroborated by X-ray diffraction (XRD) and H_2 temperature-programmed reduction (H_2-TPR) measurements. The XRD patterns (see Figure S5 in the Supporting Information) show typical Fe_3O_4 patterns of all Ir/Fe catalysts after reduction at 200 °C for 30 min. Prior to reduction they are all amorphous. As shown in Figure S6 and Table S5 in the Supporting Information, the TPR spectra are composed of

low- and high-temperature peaks. The amount of H_2 consumption related to the low-temperature peak centered at about 108 °C (T_α) is 1842 μmol g^{-1}_{cat} for Ir/Fe-UC, which is approximately eight times higher than that required for reducing Ir^{4+} to Ir^0, indicating that not only Ir^{4+} but also Fe^{3+} species are reduced at this temperature. This suggests that Ir interacts strongly with the support and there is an electron transfer between them, which is consistent with a higher binding energy (BE) of reduced Ir ($BE_{4f7/2} = 61.5$ eV, see Table S1 in the Supporting Information) than that of Ir metal ($BE_{4f7/2} = 60.2$ eV).[7b] Increasing the calcination temperature shifts T_α to a higher temperature, whereas T_β is always around 660 °C. This indicates that the calcination pre-treatment mainly affects the reducibility of the iron oxide neighbored by Ir, that is, the lower the calcination temperature, the easier the iron oxide neighbored by Ir is reduced. It has been suggested that the enhancement of surface oxygen reducibility at the metal–support interfaces determines the particularly high activity for the oxidation of CO.[22] Therefore, the slightly lower activity of Ir/Fe-C4 may be due to its lower reducibility of surface oxygen.

Imaging by HAADF-STEM technique with sub-Ångström resolution (Figure 2b) clearly shows that Ir species are uniformly dispersed over the support and exist as small clusters with sizes ≤ 1 nm. By examining various regions at different magnifications (see Figure S4 in the Supporting Information), we did not detect any Ir nanoparticles with sizes > 2 nm, which suggests that the support of $Fe(OH)_x$ or Fe_3O_4 should play an important role in stabilizing the Ir particles so that no significant aggregation takes place.

The above results show that the Ir/$Fe(OH)_x$ catalysts possess extremely high activity for the PROX reaction as well as for the oxidation of CO. The XRD, HRTEM, HAADF-STEM, XPS, and H_2-TPR characterizations indicate that the Ir species are highly dispersed on/into and strongly interact with the $Fe(OH)_x$ support. However, according to our design strategy, the crucial factor contributing to the observed high activity is the promotion of O_2 activation by the special $Fe(OH)_x$ support. To prove that the catalyst works according to the design strategy, we adsorbed CO and O_2 on our catalyst and compared the results with those achieved on conventional Ir/SiO_2; microcalorimetry and in situ diffuse reflectance infrared Fourier transform spectroscopy (DRIFTS) techniques were used. As shown in Figure S7 in the Supporting Information, the adsorption heat of CO is high on the Ir/SiO_2 catalyst (140 kJ mol^{-1}), whereas it significantly decreases to 100 kJ mol^{-1} on the Ir/Fe-UC catalyst, which is favorable for the desorption of CO followed by the adsorption of O_2. On the other hand, O_2 adsorption on Ir/Fe-UC is significantly facilitated. Not only does the adsorption heat increase greatly (from 389 kJ mol^{-1} on Ir/SiO_2 to 470 kJ mol^{-1} on Ir/Fe-UC) but also the adsorption amount drastically increases by more than 25 times (from 55 μmol g^{-1}_{cat} on Ir/SiO_2 to 1460 μmol g^{-1}_{cat} on Ir/Fe-UC). The fact that the catalyst was pre-reduced at 200 °C before measurements and that the support primarily consists of Fe_3O_4, influences the observed value of 1460 μmol g^{-1}_{cat}. This influence may originate from two different sources: normal adsorption of O_2 and oxidation of Fe_3O_4. Even if the amount of oxidizing Fe_3O_4 (1078 μmol g^{-1}_{cat}) is deducted, the amount of O_2 adsorption (385 μmol g^{-1}_{cat}) is still more than seven times higher than that on Ir/SiO_2. Therefore, the presence of $Fe(OH)_x$ greatly promotes the adsorption and activation of O_2.

The in situ DRIFTS measurements further showed the important role of $Fe(OH)_x$ for the high reactivity of our catalyst. As shown in Figure S8 in the Supporting Information, the adsorption of CO on Ir/Fe-UC produces two bands centered at 2068 and 1996 cm^{-1}, which are attributed to the linear adsorption of CO on Ir and Ir–Fe interfacial sites, respectively.[15,23] After addition of O_2, these peaks do not shift but the strength of the 1996 cm^{-1} peak decreases with concurrent release of CO_2. This result shows that O_2 may not adsorb on Ir sites but most probably on the support; if O_2 adsorbs on the Ir sites, then after the addition of O_2, the Ir–CO peak would shift to higher frequency because of the decreased back-donation from Ir to CO. All these data suggest that the reaction of CO with O_2 most probably occurs according to the noncompetitive Langmuir–Hinshelwood mechanism, that is, CO adsorbs and is activated on the Ir sites whereas O_2 adsorbs on the support and the reaction then takes place at the interfaces between Ir and the support. Microcalorimetry and in situ DRIFTS results clearly indicate that, as expected, the $Fe(OH)_x$ support greatly improves the adsorption of O_2 and successfully addresses the crucial issue of activation of O_2 on the supported Ir catalyst, thereby dramatically enhancing its activity for the PROX and the oxidation of CO.

All Pt-group metals face the same problem of O_2 activation for the CO oxidation and the PROX reactions. Since our design strategy is to promote O_2 activation by use of a special support, it should be, theoretically, effective for all Pt-group metals. To test this hypothesis, we extended our work to other Pt-group metals and synthesized Pt/$Fe(OH)_x$ and Rh/$Fe(OH)_x$ catalysts. The experimental data unambiguously show that both the Pt/$Fe(OH)_x$ and Rh/$Fe(OH)_x$ catalysts can fully convert CO at room temperature (see Figure S9 in the Supporting Information). The specific rates and TOFs (see Table 1) show that, although the reactivities are slightly different depending on the various metals, they are all of the same order of magnitude relative to that of the Au/Fe_2O_3-WGC catalyst. The activity (specific rate and TOFs) of our Rh/$Fe(OH)_x$ catalyst for the PROX reaction at room temperature is comparable to that of the most active Rh/CeO_2 catalyst tested at 110 °C.[24] To our knowledge, our Rh/$Fe(OH)_x$ should be also the most active Rh-based catalyst for the PROX reaction so far. The details on the synthesis and performance of this catalyst will be reported separately. This set of experiments unequivocally shows that our design strategy is versatile for the preparation of Pt-group metals for the PROX reaction.

In summary, we have successfully designed an extremely active Ir/$Fe(OH)_x$ catalyst for the PROX reaction. The adsorption and activation of O_2 is significantly promoted by use of an appropriate support. The adsorbed O_2 reacts with the adsorbed CO at the Ir–Fe interfaces to produce CO_2 through a noncompetitive Langmuir–Hinshelwood mechanism. Compared with traditional Ir-based catalysts, the activity of our catalyst is at least one order of magnitude

higher. This catalyst shows a comparable activity level but a wider temperature range and a better tolerance to CO_2 poisoning than the Au/Fe_2O_3-WGC catalyst, which is one of the most active catalysts for the PROX reaction. Of more importance, this design strategy is general and can be extended to other Pt-group metal catalysts.

Experimental Section

The catalysts were prepared by a co-precipitation method. Under stirring at 80 °C, to a NaOH solution an aqueous mixture of H_2IrCl_6 and $Fe(NO_3)_3{\cdot}9H_2O$ was added dropwise until the pH of the final solution reaches approximately 8. After 4 h of stirring and aging, the resulting precipitate was filtered, washed with distilled water several times, and then dried at 80 °C overnight (denoted as Ir/Fe-UC) and calcined at 200 and 400 °C for 6 h (denoted as Ir/Fe-C2 and Ir/Fe-C4, respectively).

The activity measurements were carried out in a fixed-bed reactor with 100 mg of catalyst. The feed gas for CO oxidation was 1 vol% CO and 1 vol% O_2 balanced with He. For the PROX reaction, the gas was 1 vol% CO, 1 vol% O_2, and 40 vol% H_2 balanced with He. The total gas flow rate was 30 mL min^{-1}, corresponding to a space velocity of 18000 mL h^{-1} g^{-1}_{cat}. The inlet and outlet gas compositions were analyzed online by a gas chromatograph (HP 6890-TCD, TDX-01 column) using He as the carrier gas.

Specific reaction rates and TOFs of the Ir/Fe and Au/Fe_2O_3-WGC catalysts were measured under differential conditions by decreasing the weight of the catalyst from 100 mg to about 10 mg to ensure the conversion of CO below 20%. The conversion of CO used to calculate the TOF and reaction rate was the average of three data points obtained at 20, 40, and 60 min. The dispersion of the Ir/Fe catalyst was measured by pulse adsorption of CO, using a Micromeritics AutoChem II 2920 chemical adsorption instrument at 50 °C. The dispersion of 4.4 wt% Au/Fe_2O_3-WGC was calculated according to the relationship between the dispersion degree and particle size.

Detailed procedures for HRTEM, HAADF-STEM, H_2-TPR, XRD, adsorption microcalorimetry, and in situ DRIFTS are given in the Supporting Information.

Received: September 21, 2011
Revised: January 9, 2012
Published online: February 3, 2012

Keywords: carbon monoxide · ferric hydroxide · heterogeneous catalysis · iridium · oxidation

[1] C. Song, *Catal. Today* **2002**, *77*, 17 – 49.
[2] a) V. A. Goltsov, T. N. Veziroglu, *Int. J. Hydrogen Energy* **2001**, *26*, 909 – 915; b) S. Jiménez, J. Soler, R. X. Valenzuela, L. Daza, *J. Power Sources* **2005**, *151*, 69 – 73.
[3] a) O. Korotkikh, R. Farrauto, *Catal. Today* **2000**, *62*, 249 – 254; b) D. L. Trimm, *Appl. Catal. A* **2005**, *296*, 1 – 11.
[4] a) R. M. Torres Sanchez, A. Ueda, K. Tanaka, M. Haruta, *J. Catal.* **1997**, *168*, 125 – 127; b) M. M. Schubert, A. Venugopal, M. J. Kahlich, V. Plzak, R. J. Behm, *J. Catal.* **2004**, *222*, 32 – 40; c) B. Schumacher, Y. Denkwitz, V. Plzak, M. Kinne, R. J. Behm, *J. Catal.* **2004**, *224*, 449 – 462; d) P. Landon, J. Ferguson, B. E. Solsona, T. Garcia, A. F. Carley, A. A. Herzing, C. J. Kiely, S. E. Golunski, G. J. Hutchings, *Chem. Commun.* **2005**, 3385 – 3387.
[5] S. H. Oh, R. M. Sinkevitch, *J. Catal.* **1993**, *142*, 254 – 262.
[6] a) A. Fukuoka, J. i. Kimura, T. Oshio, Y. Sakamoto, M. Ichikawa, *J. Am. Chem. Soc.* **2007**, *129*, 10120 – 10125; b) E. Y. Ko, E. D. Park, H. C. Lee, D. Lee, S. Kim, *Angew. Chem.* **2007**, *119*, 748 – 751; *Angew. Chem. Int. Ed.* **2007**, *46*, 734 – 737; c) S. Alayoglu, A. U. Nilekar, M. Mavrikakis, B. Eichhorn, *Nat. Mater.* **2008**, *7*, 333 – 338; d) Q. Fu, W. X. Li, Y. Yao, H. Liu, H. Y. Su, D. Ma, X. K. Gu, L. Chen, Z. Wang, H. Zhang, B. Wang, X. Bao, *Science* **2010**, *328*, 1141 – 1144; e) Y. Minemura, S. Ito, T. Miyao, S. Naito, K. Tomishige, K. Kunimori, *Chem. Commun.* **2005**, 1429 – 1431.
[7] a) R. Burch, *Catal. Today* **1997**, *35*, 27 – 36; b) M. Okumura, N. Masuyama, E. Konishi, S. Ichikawa, T. Akita, *J. Catal.* **2002**, *208*, 485 – 489; c) Q. Fu, T. Wagnera, *Surf. Sci. Rep.* **2007**, *62*, 431 – 498.
[8] a) F. Mariño, C. Descorme, D. Duprez, *Appl. Catal. B* **2004**, *54*, 59 – 66; b) Y. Q. Huang, A. Q. Wang, X. D. Wang, T. Zhang, *Int. J. Hydrogen Energy* **2007**, *32*, 3880 – 3886; c) W. Zhang, A. Wang, L. Li, X. Wang, T. Zhang, *Catal. Today* **2008**, *131*, 457 – 463.
[9] E. G. Derouane, *CATTECH* **2001**, *5*, 214 – 225.
[10] a) M. Haruta, *J. Nanopart. Res.* **2003**, *5*, 3 – 4; b) P. Sonström, D. Arndt, X. Wang, V. Zielasek, M. Bäumer, *Angew. Chem.* **2011**, *123*, 3974 – 3978; *Angew. Chem. Int. Ed.* **2011**, *50*, 3888 – 3891.
[11] a) M. Shou, K. Tanaka, K. Yoshioka, Y. Moro-oka, S. Nagano, *Catal. Today* **2004**, *90*, 255 – 261; b) X. Liu, O. Korotkikh, R. Farrauto, *Appl. Catal. A* **2002**, *226*, 293 – 303.
[12] W. Zhang, Y. Huang, J. Wang, K. Liu, X. Wang, A. Wang, T. Zhang, *Int. J. Hydrogen Energy* **2010**, *35*, 3065 – 3071.
[13] a) K. Liu, A. Wang, W. Zhang, J. Wang, Y. Huang, X. Wang, J. Shen, T. Zhang, *Ind. Eng. Chem. Res.* **2010**, *50*, 758 – 766; b) K. Liu, A. Wang, W. Zhang, J. Wang, Y. Huang, J. Shen, T. Zhang, *J. Phys. Chem. C* **2010**, *114*, 8533 – 8541.
[14] a) G. Smit, S. Zrncevic, K. Lazar, *J. Mol. Catal. A* **2006**, *252*, 103 – 106; b) A. A. Herzing, C. J. Kiely, A. F. Carley, P. Landon, G. J. Hutchings, *Science* **2008**, *321*, 1331 – 1335.
[15] B. Qiao, A. Wang, X. Yang, L. F. Allard, Z. Jiang, Y. Cui, J. Liu, J. Li, T. Zhang, *Nat. Chem.* **2011**, *3*, 634 – 641.
[16] P. Li, D. E. Miser, S. Rabiei, R. T. Yadav, M. R. Hajaligol, *Appl. Catal. B* **2003**, *43*, 151 – 162.
[17] a) B. Qiao, L. Liu, J. Zhang, Y. Deng, *J. Catal.* **2009**, *261*, 241 – 244; b) L. Liu, F. Zhou, L. Wang, X. Qi, F. Shi, Y. Deng, *J. Catal.* **2010**, *274*, 1 – 10.
[18] Y. Q. Huang, A. Q. Wang, L. Li, X. D. Wang, D. S. Su, T. Zhang, *J. Catal.* **2008**, *255*, 144 – 152.
[19] M. Haruta, N. Yamada, T. Kobayashi, S. Iijima, *J. Catal.* **1989**, *115*, 301 – 309.
[20] a) O. Pozdnyakova-Tellinger, D. Teschner, J. Krohnert, F. C. Jentoft, A. Knop-Gericke, R. Schlögl, A. Wootsch, *J. Phys. Chem. C* **2007**, *111*, 5426 – 5431; b) K. Tanaka, M. Shou, H. He, X. Shi, X. Zhang, *J. Phys. Chem. C* **2009**, *113*, 12427 – 12433.
[21] O. Pozdnyakova, D. Teschner, A. Wootsch, J. Kröhnert, B. Steinhauer, H. Sauer, L. Toth, F. C. Jentoft, A. Knop-Gericke, Z. Paál, R. Schlögl, *J. Catal.* **2006**, *237*, 1 – 16.
[22] a) A. M. Venezia, G. Pantaleo, A. Longo, G. Di Carlo, M. P. Casaletto, F. L. Liotta, G. Deganello, *J. Phys. Chem. B* **2005**, *109*, 2821 – 2827; b) Y. N. Sun, Z. H. Qin, M. Lewandowski, E. Carrasco, M. Sterrer, S. Shaikhutdinov, H. J. Freund, *J. Catal.* **2009**, *266*, 359 – 368.
[23] F. Solymosi, J. Raskó, *J. Catal.* **1980**, *62*, 253 – 263.
[24] D. A. J. M. Ligthart, R. A. van Santen, E. J. M. Hensen, *Angew. Chem.* **2011**, *123*, 5418 – 5422; *Angew. Chem. Int. Ed.* **2011**, *50*, 5306 – 5310.

